DOI 10.1007/s10891-018-1770-7

Journal of Engineering Physics and Thermophysics, Vol. 91, No. 1, January, 2018

EXPERIMENTAL INVESTIGATION OF THE THERMOPHYSICAL PROPERTIES OF TiO_2/PROPYLENE GLYCOL–WATER NANOFLUIDS FOR HEAT-TRANSFER APPLICATIONS

M. Leena and S. Srinivasan

UDC 541.182

Nanofluids have been prepared by dispersing TiO_2 nanoparticles in 70:30% (by weight) water–propylene glycol mixture. The thermal conductivity and viscosity were found experimentally at various temperatures with the volume concentrations 0.1–0.8%. The results indicate that the thermal conductivity of the nanofluids increases with the volume concentration and temperature. Similarly, the viscosity of the nanofluids increases with the volume concentration but decreases with increase in the temperature. Correlations have been proposed for estimating the thermal conductivity and viscosity of the nanofluids. The potential heat transfer benefits of their use in laminar and turbulent flow conditions has been explained.

Keywords: *TiO_2 nanofluids, thermal conductivity enhancement, viscosity, density, volume concentration.*

Introduction. Water, oils, and glycol as traditionally used heat-transfer fluids play a vital role in the energy saving systems. These fluids are widely used in refrigerators, air conditioning, transportation, as well as in solar thermal and electronics industries. However, these conventional fluids have limited heat-transfer capabilities. Therefore, a number of researches were focused on enhancing the thermal properties to improve the energy efficiency of the systems [1–3]. The use of heat-transfer fluids of lower viscosity and higher thermal conductivity is one of the ways of improving the efficiency of thermal management systems. It is well established that a suspension of solid particles in a base fluid increases the thermal conductivity and offers a great potential for enhanced heat transfer [4]. Microsized solid particles have been used to prepare a dispersion whose rapid settling leads to precipitation abrasion and clogging.

Nanofluids, which contain nanoparticles dispersed in a base fluid, are promising candidates for heat-transfer fluids owing to their higher thermal conductivity in comparison to that of conventional fluids. Due to the higher colloidal stability and higher surface volume ratio, nanofluids are better heat-transfer fluids than those containing milli- or micrometer particles [5–12]. Metal oxides are preferred for the nanofluid preparation owing to their chemical stability and easiness of handling. A significant number of researches were devoted to nanofluids containing TiO_2 due to their high stability, low cost, and environmentally benign nature [13]. Duangthongsuk and Wongwises [14] studied the temperature-dependent viscosity and thermal conductivity of TiO_2–water nanofluids. Tseng and Wu [15] investigated the rheology and colloidal structure of aqueous TiO_2 nanoparticle suspensions. He et al. [16] showed that addition of TiO_2 to a base liquid rases the thermal conductivity, which increases with the particle concentration and with decrease in the particle size. The results of Kim, Choi, and Kim [17] showed the increase in the thermal conductivity with reduction in the particle size. Yoo, Hong, and Yang [18] found that a titania nanofluid was characterized by large enhancement of the thermal conductivity compared to that of base fluids.

We have synthesized TiO_2 nanoparticles by the sol-gel method. It is one of the most used methods due to a possibility of obtaining a unique metastable structure at low reaction temperatures and an excellent chemical homogeneity [19]. This paper is aimed at measuring the thermal conductivity, viscosity, and the density of TiO_2/water–propylene glycol mixture (70:30%) nanofluids at various particle volume concentrations and temperatures. The results are used to correlate the physical properties with the thermal behavior of the nanofluids for estimating their viability for industrial applications.

Experimental Details. Nanofluids can be prepared by a two-step method: first they are produced as a dry powder, which then is dispersed in a fluid.

Preparation of nanofluids. TiO_2 nanoparticles were prepared by the sol-gel method, using titanium (IV) isopropoxide (TTIP) as a precursor. TTIP was obtained from Sigma Aldrich Company, USA with a stated purity of 97%. It was dropped

Department of Physics, Presidency College (Autonomous), Chennai-600005, India; email: leerithima@hotmail.com.
Published in Inzhenerno-Fizicheskii Zhurnal, Vol. 91, No. 2, pp. 525–533, March–April, 2018. Original article submitted November 6, 2015; revision submitted June 20, 2017.

slowly into a mixed solution of ethanol and distilled water in the stoichiometry ratio 1:4:1 (TTIP/H_2O/ethanol). The solution was continuously stirred for 1 h at room temperature, and a white slurry solution was obtained. Nitric acid was used to obtain the pH in the range 2–3. After aging for 24 h, the solution was transformed into a gel. The gel was dried at a temperature under 120°C for 2 h to evaporate water and waste organic materials. Finally the dry gel was sintered at 450°C for 2 h to obtain a TiO_2 nanopowder. The amount of TiO_2 nanoparticles required for the preparation of a nanofluid with a particular concentration is estimated as the ratio of the volume of TiO_2 to the sum of this volume and the base fluid volume.

TiO_2 nanoparticles were dissolved in propylene glycol and distilled water in the volume ratio 30:70. Three fluids with different concentrations of TiO_2 nanoparticles ranging from 0.1 to 0.8 vol.% were prepared. The test samples were ultrasonicated for 4 h to prevent agglomeration. No surfactant was added, because it reduces the thermal conductivity of nanofluids, as was observed in the experiments [20].

Characterization. The X-ray diffraction analysis of the TiO_2 nanoparticle powder was carried out by using a Seifert XRD Rigaker D/Max 2500V diffractometer equipped with a diffracted beam monochromator operating at the voltage 40 kV and the current 450 mA. The average nanoparticle size was determined from the Debye–Scherrer relation:

$$D = \frac{K\lambda}{\beta \cos \theta},$$

where K is the shape factor ($K = 0.89$), λ is the X-ray wavelength ($\lambda = 1.54$ Å), β is the peak broadening at half the maximum intensity, and θ is the Bragg angle. The surface morphology and elemental analysis of the prepared nanoparticles were performed by a high-resolution scanning electron microscope (HRSEM) FEI QUNTA FEG 200 fitted with an energy dispersive X-ray spectroscope EDAX Genesis 4000. UV-visible spectral measurements were carried out to determine the relative stability of nanofluids in the wavelength range 190–900 nm. The densities of both the water–propylene glycol mixture and nanofluids were measured at 298.15 K, using a specific gravity bottle (5 mL), by the relative measurement method. The sample weight was measured by an electronic digital balance with an accuracy of ±0.1 mg (Model Shimadzu ELB 300). An RVDV-E viscometer was used to measure the viscosity of TiO_2 nanofluids at various particle concentrations and temperatures. The viscosity measurements were started at 50°C, and then the temperature was gradually reduced to 10°C. The uncertainty of these measurements was ±1% of a full-scale range. The increase in the thermal conductivity was determined at different volume fractions and the temperatures 30–70°C, using a Netzsch LFA 447 Nano LFA technique (LFA is the laser flash analysis). The uncertainty of the measurements of the thermal diffusivity was ±1% and of the specific heat, ±5%.

Results and Discussion. *Structural and morphological studies.* The X-ray diffraction (XRD) pattern of synthesized TiO_2 nanoparticles at 450°C is shown in Fig. 1. The high-intensity peak (101) at $2\theta = 25.4^o$ is consistent with the anatase phase [21] of TiO_2, matches well with the standard Joint Committee on Powder Diffraction Standards file No. 21-1272, and belongs to a cubic system. The crystallite size was determined for the most intense XRD peak (101), using the Scherrer formula, and it was found to be 20 nm. Figure 2 shows the high-resolution sem-scanning electron microscope (HRSEM) image of TiO_2 nanoparticles. It was found that the nanoparticles show spherical morphology, and the particle size was found to be 20 nm. Energy-dispersive spectroscopy (EDS) identifies the elements and their relative proportions in the given sample. The elemental analysis of the synthesized TiO_2 nanomaterial showed that the required concentrations of titanium (73%) and oxygen (27%) were present in the sample at 450°C, and there was no trace of any foreign impurity within the detectable limits of the EDS.

UV absorption study. UV-visible spectral analysis was employed to study the dispersion stability of the prepared nanofluid samples. After 4 h sonication, TiO_2 nanofluids with 0.1, 0.4, and 0.8 vol.% fractions were stable for more than 28, 10, and 7 h, respectively. The spectra were recorded up to 900 nm, as shown in Fig. 3. We observe the slight shift towards smaller wavelengths and the decrease in the absorbance of ultraviolet rays, which is attributed to the decrease in the percent loading of TiO_2 nanoparticles and to dispersion of TiO_2 nanofluids.

The direct band gap energy E_g of the samples was determined by fitting the absorption data to the following equation:

$$\alpha h\nu = A(h\nu - E_g)^{1/2}, \quad (1)$$

where α is the optical absorption coefficient, h is the Planck constant, ν is the frequency, and A is constant. The band gap energy E_g of the as-prepared TiO_2 nanoparticles is larger than the value 3.2 eV for bulk TiO_2 due to the contribution of the quantum size effect [22]. When the concentration increases, the band gap energy gradually decreases from 3.63 to 2.7 eV, as

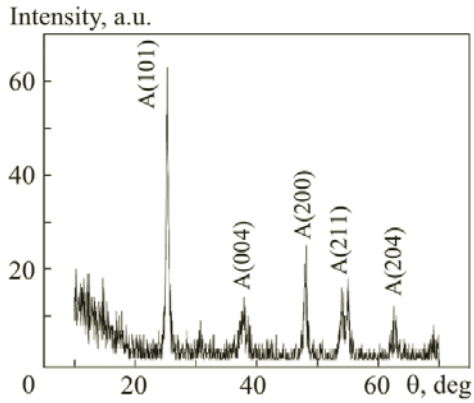

Fig. 1. X-ray diffraction pattern of TiO_2 nanoparticles.

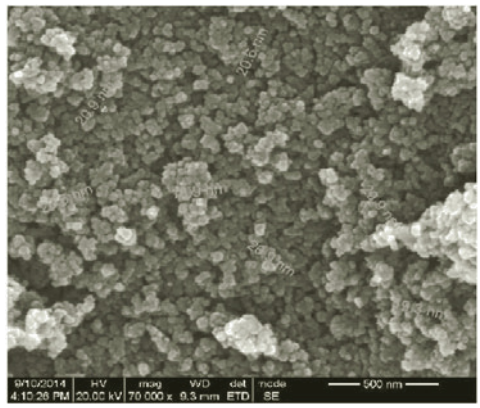

Fig. 2. HRSEM morphology of TiO_2 nanoparticles.

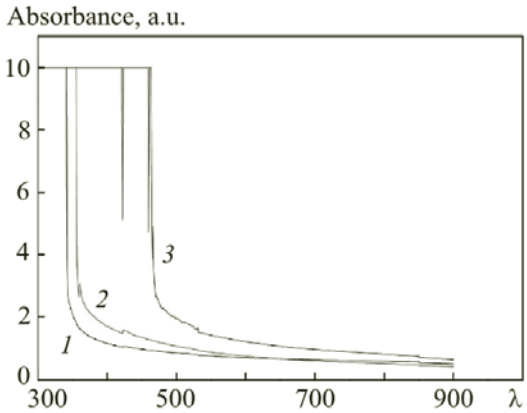

Fig. 3. UV-visible absorption spectra of TiO_2/water–propylene glycol nanofluids at different concentrations of TiO_2 nanoparticles: 0.1 (1), 0.4 (2), and 0.8 vol.% (3).

seen in Fig. 4. At the high concentration 0.8%, the band gap energy has the lowest value (~3 eV), because the particle size becomes bigger. Therefore, when the particle size increases, the stability gradually decreases.

Density of TiO_2 nanofluids. The density of water–propylene glycol-based nanofluids is determined as

$$\rho_{nf} = \frac{m_t - m_b}{V_{nf}}, \tag{2}$$

where m_t and m_b are the total mass of the bottle with the nanofluid and the mass of the empty bottle, respectively. The experimentally obtained density data are compared with the density obtained from the correlation proposed by Pak and Cho [23]:

$$\rho_{nf} = \phi\rho_p + (1 - \phi)\rho_{bf} . \tag{3}$$

To confirm the validity of the Pak and Cho model, we measured the density of the TiO_2/water–propylene glycol mixture at room temperature. From Fig. 5 it is seen that the model underpredicts the density values by 11, 19, and 36 $kg \cdot m^{-3}$, when the nanofluid contains 0.1, 0.4, and 0.8% of TiO_2 nanoparticles, respectively. It was observed that the predicted value increases with the concentration of TiO_2. The mentioned difference may be attributed to spontaneous filling of TiO_2 nanoparticles with the water–propylene glycol mixture in a confined way, which increases the nanofluid mass for a given volume [24].

Viscosity of TiO_2 nanofluids. Different theoretical models predict the effective viscosity of solid–fluid mixtures. Drew and Passman [25] used the well-known Einstein model [26] for evaluating the effective viscosity of a linearly viscous fluid of viscosity μ_{bf} containing a dilute suspension of spherical particles. The viscosity according to the Einstein model is

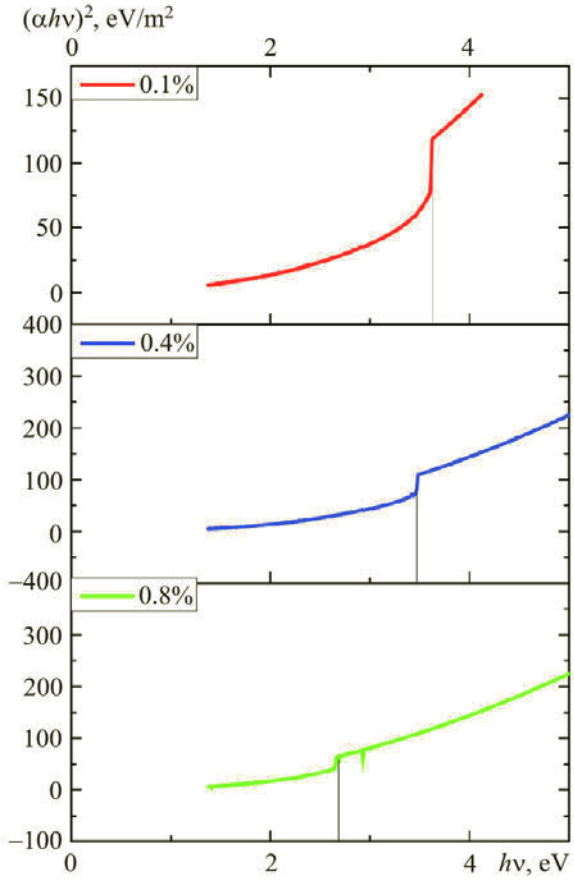

Fig. 4. Values of $(\alpha h\nu)^2$ vs. $h\nu$.

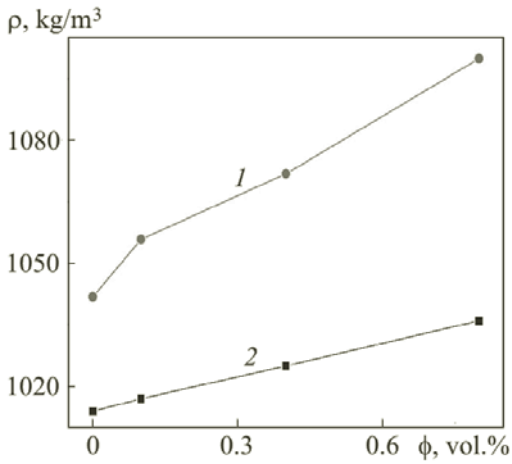

Fig. 5. Nanofluid density of TiO_2 nanofluid vs. the concentration: experiment (1) and data of [23] (2).

$$\mu_{nf} = (1 + 2.5\phi)\mu_{bf} \ . \tag{4}$$

This formula was found to be applicable to relatively low particle volume fractions ($\phi < 0.05\%$). There exists the extended Einstein formula proposed by Brinkman [27] for moderate particle concentrations:

$$\mu_{nf} = (1 + 2.5\phi + 4.375\phi^2 + ...)\mu_{bf} \ . \tag{5}$$

Fig. 6. RVDV-E viscometer for measurement of the TiO_2 nanofluid viscosity.

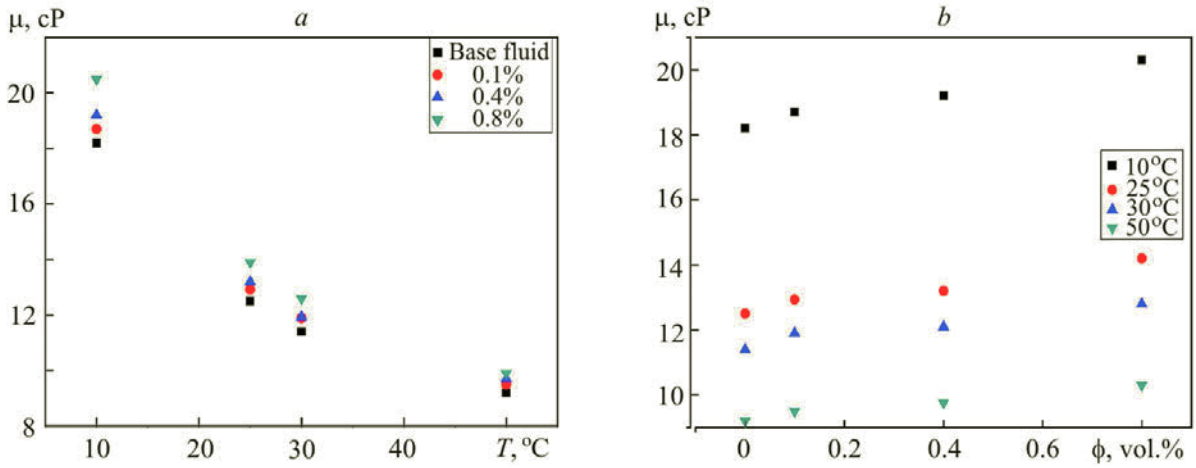

Fig. 7. Viscosity of TiO_2 nanofluid vs. the temperature at different concentrations (a) and vs. the concentration at different temperatures (b).

Batchelor [28] proposed the following equation for an approximately isotropic suspension of rigid and spherical particles, considering the effect of Brownian motion of particles on the bulk stress:

$$\mu_{nf} = (1 + 2.5\phi + 6.2\phi^2)\mu_{bf} \ . \tag{6}$$

An RVDV-E viscometer (Fig. 6) was calibrated with 70:30% W/PG (water/propylene glycol), and the obtained data are shown in Fig. 7. It is observed that the viscosity of nanofluids increases with the particle volume concentration but decreases with

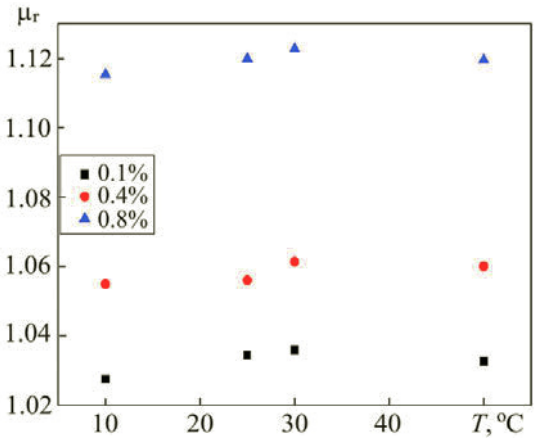

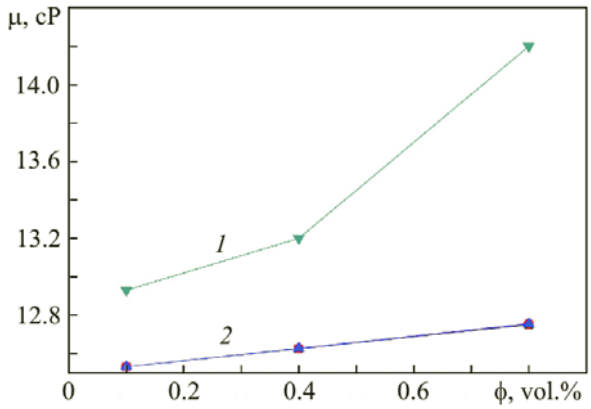

Fig. 8. Viscosity ratio of TiO_2 nanofluid vs. the temperature at different concentrations.

Fig. 9. Viscosity of TiO_2 nanofluid vs. the concentration according to experiment (1) and model correlations (2).

increase in the temperature as compared to that of the base fluid. This effect is due to the fact that an increase in the temperature decreases the intermolecular forces between TiO_2 nanoparticles and base fluid [29]. The viscosity ratio $\mu_r = \mu_{nf}/\mu_{bf}$ at the temperature 10°C was 1.0275, 1.0549, and 1.1154 for 0.1, 0.4, and 0.8 vol.% concentrations, respectively. Nanofluids prepared with high-viscosity base fluids exhibit more enhancement compared to low-viscosity ones. Figure 8 presents the viscosity ratio versus the temperature at various concenations. The ratio generally increases with the concentration of TiO_2 nanoparticles. At the lowest concentration 0.1% the ratio shows a weak dependence on the temperature; however, it is greatly influenced by the temperature at higher concentrations. At lower temperatures, particularly at 10°C, the viscosity ratio is low for all the nanofluids, which makes them suitable for cooling applications with minimum penalty in the pumping power. However, the increase in the viscosity ratio at high temperatures will certainly attenuate the positive thermal transport effects, predominantly in the area of convective heat transfer.

Dispersion of nanoparticles in base fluids causes the development of the resistance between the fluid layers and helps to enhance the viscosity. This phenomenon was observed in all the base fluids. In the present analysis, the viscosity of nanofluids subject to the effect of base fluids indicates that pure PG-based nanofluids provided larger viscosity than the 70:30% W/PG-based nanofluids at the measured particle loadings and temperatures.

Various base fluids, particle sizes, and preparation methods are among the reasons for obtaining different viscosity ratios. The classical theoretical models, such as those of Einstein [26], Brinkman [27], and Batchelor [28], give almost the same value of the viscosity, as can be seen in Fig. 9, but all these models underpredict the experimental results. This may be due to the fact that the models do not account for the nanoparticle shape and size.

Thermal conductivity of TiO_2 nanofluids. The enhancement of the thermal conductivity was determined at different volume fractions and temperatures (30–70°C), using a Netzsch LFA 447 Nano LFA technique (see Fig. 10). The LFA is a direct measurement method for determining the thermal diffusivity and an indirect method for determining the thermal conductivity. Nanofluids with different volume concentrations were introduced into the apparatus. The obtained data for 70:30% W/PG nanofluids are presented in Fig. 11 along with the data for the base fluid. It is seen that the thermal conductivity of the nanofluids increases with the volume concentration and temperature. While the heat transfer enhancement with using nanoparticles depends on the flow conditions, such a tendency can be attributed to different reasons, like Brownian motion, nanolayering, and the effect of particles clustering [30, 31]. At a temperature of 25°C and concentrations 0.1 and 0.8 vol.% the enhancement of the thermal conductivity was 5.45 and 7.57%. At a temperature of 70°C such an enhancement was 21.44 and 48.84%. The reasons for the enhancement of the thermal conductivity consist of Brownian motion and microconvection of particles in the base fluids. This enhancement depends not only on the particle concentration and temperature, but also on the base fluid effect.

Heat transfer of TiO_2 nanofluids in laminar flow. Low-viscosity fluids are more advantageous in industrial applications. To predict the potentialities of nanofluids in actual applications, the relative coefficients of the thermal conductivity and viscosity enhancement in laminar flow conditions were proposed by Prasher et al. [32] as

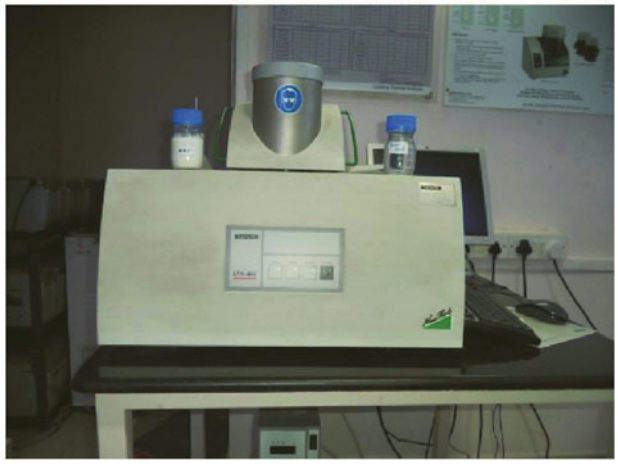

Fig. 10. Laser flash apparatus.

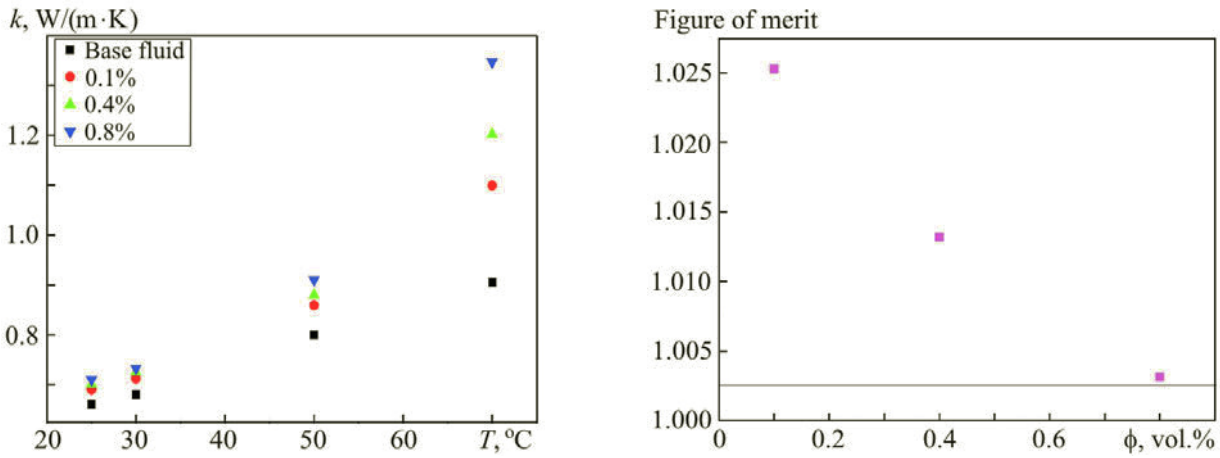

Fig. 11. Thermal conductivity ratio of TiO_2 nanofluid vs. the temperature at different concentrations.

Fig. 12. Figure of merit of TiO_2 nanofluid at $T = 30^{o}C$ and different concentrations.

$$\frac{\mu_{nf}}{\mu_{bf}} = 1 + C_{\mu}\phi \,, \tag{7}$$

$$\frac{k_{nf}}{k_{bf}} = 1 + C_{k}\phi \,, \tag{8}$$

where C_{μ} and C_k are the viscosity and thermal conductivity enhancement coefficients. According to [32], a nanofluid is beneficial if $C_{\mu}/C_k < 4$. From Eqs. (7) and (8), for 70:30% W/PG nanofluid at 25°C and 0.8 vol.% concentration $C_{\mu} = 14.0$ and $C_k = 9.47$, i.e., $C_{\mu}/C_k = 1.5$. Thus, 70:30% W/PG nanofluid is beneficial in a fully developed laminar flow due to its low viscosity.

Heat transfer of TiO_2 nanofluids in turbulent flow. The Mouromtseff number Mo can be used to compare two fluids in turbulent flow conditions. In the experimental determination of the viscosity and thermal conductivity, the theoretical values of the density and specific heat were used to evaluate the thermal effectiveness of a nanofluid through the Mouromtseff number [33]. A figure of merit (FOM) is used to evaluate and compare the heat transfer capabilities of fluids. Higher values of Mo correspond to higher heat transfer capability of the fluid for a given geometry at a specified velocity. We have

$$\mathrm{Mo}_{\mathrm{nf}} = \frac{\rho_{\mathrm{nf}}^{0.8} k_{\mathrm{nf}}^{0.67} C_{p,\mathrm{nf}}^{0.33}}{\mu_{\mathrm{nf}}^{0.47}}, \tag{9}$$

$$\mathrm{Mo}_{\mathrm{bf}} = \frac{\rho_{\mathrm{bf}}^{0.8} k_{\mathrm{bf}}^{0.8} C_{p,\mathrm{bf}}^{0.33}}{\mu_{\mathrm{bf}}^{0.47}}, \tag{10}$$

$$\mathrm{FOM} = \frac{\mathrm{Mo}_{\mathrm{nf}}}{\mathrm{Mo}_{\mathrm{bf}}}. \tag{11}$$

The value FOM > 1 provides higher-heat transfer benefits at the same velocity for a particular system. Figure 12 presents a figure of merit for 70:30% W/PG nanofluids at different volume concentrations and a temperature of 30°C. It is seen that for all volume concentrations FOM > 1. This indicates that the nanofluids prepared with 70:30% W/PG was less viscous. Hence, these nanofluids are suitable for the use as heat-transfer fluids in turbulent flow conditions. However, the Mouromtseff number does not incorporate any additional heat-transfer mechanisms that have been described in the studies on nanofluid heat transfer. Therefore, the additional experiments on the fluid potential should be conducted.

Conclusions. Experimental analysis was conducted for estimating the density, viscosity, and thermal conductivity of a TiO_2 nanofluid with consideration for the influence of the particle concentration, temperature, and the properties of a base fluid. It is shown that the nanofluid density increases with the volume concentration of TiO_2 nanoparticles. The measurement data show an observable deviation from the predicted values based on the Pak and Cho correlation, and this deviation increases with the TiO_2 concentration. This is due to spontaneous filling of TiO_2 nanoparticles with a base fluid in a confined way, which in turn increases the nanofluid mass for a given volume.

The thermal conductivity enhancement depends on the particle volume concentration and temperature. For 0.8 vol.% concentration, the enhancement in the thermal conductivity for the temperature range 25–70° comprised 7.57–48.84%.

The viscosity enhancement for 0.8% vol.% concentration in 70:30% W/PG nanofluid at a temperature of 10°C was 1.1154. Nanofluids prepared with higher-viscosity base fluids exhibit higher enhancement compared to low-viscosity ones. The temperature effect on the viscosity and thermal conductivity was also examined. Based on the thermal conductivity and viscosity data, a preliminary estimation of the potential of the considered nanofluid system has been made.

Acknowledgments. The authors would like to express their sincere thanks to SAIF, IIT-Madras, Chennai for providing HRSEM and the Department of Nuclear Physics, University of Madras, Chennai for providing XRD analysis.

NOTATION

C_p, specific heat; k, thermal conductivity; m, mass; T, temperature; V, volume; μ, viscosity; ρ, density; ϕ, volume fraction. Indices: b, bottle; bf, base fluid; nf, nanofluid; p, particles; t, total.

REFERENCES

1. U. S. Choi, Y. I. Cho, and K. E. Kasza, Degradation effects of dilute polymer solutions on turbulent friction and heat transfer behavior, *J. Non-Newtonian Fluid Mech.*, **41**, 289–307 (1992).
2. U. S. Choi, D. M. France, and B. D. Knodel, Impact of advanced fluids on costs of district cooling systems, in: *Proc. 83rd Ann. Int. District Heating and Cooling Association Conf.*, Danvers, Washington, D. C. (1992), pp. 343–359.
3. V. Bianco, O. Manca, and S. Nardini, Numerical simulation of water/nanofluid turbulent convection, *Adv. Mech. Eng.*, **2**, 1–10 (2010).
4. Y. Touloukian, *Thermal Conductivity: Nonmetallic Liquids and Gases (Thermophysical Properties of Matter)*, Springer, New York (1970).
5. S. U. S. Choi and J. A. Eastman, Enhancing thermal conductivity of fluids with nanoparticles, in: *Proc. ASME Int. Mechanical Engineering Congress and Exposition*, San Francisco (1995), pp. 99–105.
6. X. Q. Wang and A. S. Mujumdar, Heat transfer characteristics of nanofluids: A review, *Therm. Sci.*, **46**, 1–19 (2007).
7. J. A. Eastman, S. U. S. Choi, S. Li, W. Yu, and L. J. Thompson, Anomalously increased effective thermal conductivities of ethylene glycol-based nanofluids containing copper nanoparticles, *Appl. Phys. Lett.*, **78**, 718–720 (2001).

8. K. S. Hong, T. K. Hong, and H. S. Yang, Thermal conductivity of Fe nanofluids depending on the cluster size of nanoparticles, *Appl. Phys. Lett.*, **88**, 031901–031903 (2006).
9. D. Hemanth Kumar, H. E. Patel, V. R. R. Kumar, T. Pradeep, and S. K. Das, Model for heat conduction in nanofluids, *Phys. Rev. Lett.*, **93**, 144301–144304 (2004).
10. S. Lee, S. U. S. Choi, S. Li, and J. A. Eastman, Measuring thermal conductivity of fluids containing oxide nanoparticles, *Heat Transf.*, **121**, 280–289 (1999).
11. Y. Xuan and Q. Li, Heat transfer enhancement of nanofluids, *Heat Fluid Flow*, **21**, 58–64 (2000).
12. J. Jeong, C. Li, Y. Kwon, J. Lee, S. H. Kim, and R. Yun, Particle shape effect on the viscosity and thermal conductivity of ZnO nanofluids, *Int. J. Refrig.*, **36**, 2233–2241 (2013).
13. A. Ghadimi and I. H. Metselaar, The influence of surfactant and ultrasonic processing on improvement of stability, thermal conductivity and viscosity of titania nanofluid, *Exp. Therm. Fluid Sci.*, **51**, 1–9 (2013).
14. W. Duangthongsuk and S. Wongwises, Measurement of temperature-dependent thermal conductivity and viscosity of TiO_2-water nanofluids, *Exp. Therm. Fluid Sci.*, **33**, 706–714 (2009).
15. W. J. Tseng and C. H. Wu, Aggregation, rheology and electrophoretic packing structure of aqueous Al_2O_3 nanoparticle suspensions, *Acta Mater.*, **50**, 3757–3766 (2002).
16. Y. He, Y. Jin, H. Chen, Y. Ding, D. Cang, and H. Lu, Heat transfer and flow behaviour of aqueous suspensions of TiO_2 nanoparticles (nanofluids) flowing upward through a vertical pipe, *Heat Mass Transf.*, **50**, 2272–2281 (2007).
17. S. H. Kim, S. R. Choi, and D. Kim, Thermal conductivity of metal-oxide nanofluids: particle size dependence and effect of laser irradiation, *Heat Transf.*, **129**, 298–307 (2006).
18. D. H. Yoo, K. S. Hong, and H. S. Yang, Study of thermal conductivity of nanofluids for the application of heat transfer fluids, *Thermochim.* Acta, **455**, 66–69 (2007).
19. S. A. Ibrahim and S. Sreekantan, Effect of pH on TiO_2 nanoparticles via sol-gel method, in: *Proc. ICXRI*, 9–10 June, 2010, Aseania Resort Langkawi, Malaysia (2010), pp. 84–87.
20. K. D. Kihm, Fundamendals of energy transport in nanofluids, *Annual Report*, 1–42 (2003).
21. Y. Zhao, C. Li, X. Liu, F. Gu, H. Jiang, W. Shao, L. Zhang, and Y. Ge, Synthesis and optical properties of TiO_2 nanoparticles, *Mater. Lett.*, **61**, 79–83 (2007).
22. K. M. Reddy, S. V. Manorama, and A. Ramachandra Reddy, Bandgap studies on anatase titanium dioxide nanoparticles, *Mater. Chem. Phys.*, **78**, 239–245 (2002).
23. B. C. Pak and Y. I. Cho, Hydrodynamic and heat transfer study of dispersed fluids with submicron metallic oxide particles, *Exp. Heat Transf.*, **11**, 151–170 (1999).
24. Z. Haddad, C. Abid, O. Rahil, O. Margeat, W. Dachraoui, and A. Mataoui, Is it important to measure the volumetric mass density of nanofluids? *Math. Phys. Electrical Comput. Eng.*, **8**, 310–313 (2014).
25. D. A. Drew and S. L. Passman, *Theory of Multicomponent Fluids*, Springer, Berlin (1999).
26. A. Einstein, Eine neue Bestimmung der Moleküldimensionen, *Ann. Phys.*, **19**, 289–306 (1906).
27. H. C. Brinkman, The viscosity of concentrated suspensions and solutions, *Chem. Phys.*, **20**, 571–580 (1952).
28. G. K. Batchelor, The effect of Brownian motion on the bulk stress in a suspension of spherical particles, *Fluid Mech.*, **83**, 97–117 (1977).
29. N. Jamshidi, M. Farhadi, D. D. Ganji, and K. Sedighi, Experimental investigation on the viscosity of nanofluids, *Eng. Transact.* B, **25**, 201–209 (2012).
30. S. M. S. Murshed, K. C. Leong, and C. Yang, Enhanced thermal conductivity of TiO_2-water based nanofluids, *Int. J. Therm.* Sci., **44**, 367–373 (2005).
31. M. Jalal, H. Meisami, and M. Pouyagohar, Experimental study of CuO/water nanofluid effect on convective heat transfer of a heat sink, *Sci. Res.*, **13**, 606–611 (2013).
32. R. Prasher, D. Song, J. Wang, and P. Phelan, Measurements of nanofluid viscosity and its implications for thermal applications, *Appl. Phys. Lett.*, **89**, 133108–1331083 (2006).
33. R. E. Simons, Comparing heat transfer rates of liquid coolants using the Mouromtseff number, *Electron. Cool.*, **12**, No. 2 (2006).